# Induced Self-Assembly and Disassembly of Water-Soluble Alkynylplatinum(II) Terpyridyl Complexes with "Switchable" Near-Infrared (NIR) Emission Modulated by Metal-Metal Interactions over Physiological pH: Demonstration of pH-Responsive NIR Luminescent Probes in Cell-Imaging Studies

*Clive Yik-Sham Chung,*[a] *Steve Po-Yam Li,*[b] *Man-Wai Louie,*[b] *Kenneth Kam-Wing Lo*[b] *and Vivian Wing-Wah Yam**[a]

[a] Institute of Molecular Functional Materials,[†] and Department of Chemistry, The University of Hong Kong, Pokfulam Road, Hong Kong, P. R. China

[b] Department of Biology and Chemistry, City University of Hong Kong, Tat Chee Avenue, Kowloon, Hong Kong, P. R. China

*To whom correspondence should be addressed. Email: wwyam@hku.hk

[†] Areas of Excellence Scheme, University Grants Committee (Hong Kong)

## Electronic Supplementary Information

## Experimental Section

**Materials and Reagents.** 2-Acetylpyridine, *p*-tolualdehyde, 2,2′-azobis(2-methylpropionitrile) (AIBN), 4-iodophenol, 3,5-dimethoxyaniline, $BBr_3$ in dichloromethane, trimethylamine (33% wt. in ethanol) and 3-(4,5-dimethyl-2-thiazolyl)-2,5-diphenyltetrazolium bromide (MTT) were purchased from Sigma-Aldrich. 4′-(*p*-Tolyl)-2,2′:6′,2″-terpyridine,[S1] 4′-(4-(bromomethyl)phenyl)-2,2′:6′,2″-terpyridine,[S2] 4-trimethylsilylethynylphenol,[S3] 1-iodo-3,5-dimethoxy-benzene,[S4] 1-iodo-3,5-dihydroxybenzene,[S4] 4-ethynylphenol,[S5] 1,3-dimethoxy-5-trimethylsilylethynylbenzene[S6] and 1-ethynyl-3,5-dimethoxybenzene[S6] were synthesized according to the reported literatures. LysoSensor Green DND-189, Dulbecco's modified Eagle's medium (DMEM), fetal bovine serum (FBS), phosphate-buffered saline at pH 7.2 (PBS), trypsin-EDTA, and penicillin/streptomycin were purchased from Invitrogen. All other reagents were of analytical grade and were used without further purification. The synthesis was performed under an inert atmosphere of nitrogen unless specified otherwise.

**Physical Measurements and Instrumentation.** $^1$H NMR spectra were recorded with a Bruker AVANCE 400 and 600 (400 and 600 MHz) or DPX-300 (300 MHz) Fourier transform NMR spectrometer at ambient temperature with tetramethylsilane ($Me_4Si$) as an internal reference. Positive ion FAB or EI mass spectra were recorded on a Thermo Scientific DFS High Resolution Magnetic Sector mass spectrometer. Elemental analyses for the metal complexes were performed on the Carlo Erba 1106 elemental analyzer at the Institute of Chemistry, Chinese Academy of Sciences, Beijing, China. IR spectra of the solid samples were obtained as Nujol mulls on KBr disks on a Bio-Rad FTS-7 Fourier transform infrared spectrophotometer (4000-400 $cm^{-1}$). UV-vis absorption spectra were recorded on a Cary 50 (Varian)

spectrophotometer equipped with a Xenon flash lamp. Steady state emission spectra were recorded using a Spex Fluorolog-3 Model FL3-211 fluorescence spectrofluorometer equipped with a R2658P PMT detector. DLS measurements of complex **1** were performed using Zetasizer 3000HSA with internal HeNe laser ($\lambda_0$ = 632.8 nm) from Malvern (UK). Unless specified otherwise, the emission spectra were corrected for PMT response.

**Syntheses.**

**4′-{4-[(Trimethylammonium)methyl]phenyl}-2,2′:6′,2″-terpyridine trifluoro-methanesulfonate ([L][OTf]).**

4′-{4-[(Trimethylammonium)methyl]phenyl}-2,2′:6′,2″-terpyridine bromide was synthesized according to the reported literature.[S7] Metathesis reaction of the bromide salt (800 mg, 1.73 mmol) with AgOTf gave the trifluoromethanesulfonate salt as an off-white solid. Yield = 600 mg (65%). $^1$H NMR (300 MHz, MeOD-$d_4$): δ = 3.20 (s, 9H), 4.67 (s, 2H), 7.36 (m, 2H), 7.84 (d, *J* = 8.3 Hz, 2H), 8.01 (m, 2H), 8.10-8.13 (m, 2 H), 8.18 (d, *J* = 8.3 Hz, 2H), 8.37 (d, *J* = 8.0 Hz, 2H), 8.54 (s, 2H). Positive FAB-MS, *m/z*: 531. Elemental analysis calcd (%) for $C_{26}H_{25}F_3N_4O_3S$: C 58.86, H 4.75, N 10.56; found: C 58.79, H 5.01, N 10.18.

**1,3-Dihydroxy-5-trimethylsilylethynylbenzene.** A mixture of 1-iodo-3,5-dihydroxybenzene (1 g, 4.23 mmol), bis(triphenylphosphine)palladium(II) chloride (148.5 mg, 0.21 mmol) and copper(I) iodide (40.28 mg, 0.21 mmol) in distilled triethylamine (20 mL) and THF (20 mL) was deaerated with nitrogen. (Trimethylsilyl)acetylene (1.24 g, 12.71 mmol) was then added to the reaction mixture and was stirred for 12 h at room temperature. After the addition of diethyl ether, the solution mixture was then filtered and the filtrate was evaporated to dryness

under reduced pressure to give a solid residue. The crude product was then purified by column chromatography on silica gel, using hexane:aceteone (3:1 *v*/*v*) as eluent. Yield = 800 mg (92 %). $^1$H NMR (300 MHz, $CDCl_3$): δ = 0.23 (s, 9H), 4.87 (s, 2H), 6.33 (s, 1H), 6.52 (s, 2H). Positive EI-MS, *m/z*: 206. HRMS (Positive EI) calcd for $C_{11}H_{14}O_2{}^{28}Si$: *m/z* = 206.0758; found: 206.0758 $[M]^+$.

**1-Ethynyl-3,5-dihydroxybenzene.** Potassium carbonate (536 mg, 3.88 mmol) was added to a solution of 1,3-dihydroxy-5-trimethylsilylethynylbenzene (200 mg, 0.97 mmol) in THF-MeOH (3:1 *v/v*) with stirring for 5 hours. The reaction mixture was then evaporated under reduced pressure. The crude product was dissolved in $CHCl_3$ and washed with water twice. The organic layer was dried over anhydrous $MgSO_4$ and evaporated under reduced pressure. The product was obtained as a pale yellow oil. Yield = 75 mg (58 %). $^1$H NMR (400 MHz, $CDCl_3$): δ = 3.02 (s, 1H), 5.17 (s, 2H), 6.37 (s, 1H), 6.64 (s, 2H). Positive EI-MS, *m/z*: 134. HRMS (Positive EI) calcd for $C_8H_6O_2$: *m/z* = 134.0362; found: 134.0363 $[M]^+$.

**[Pt(L)Cl](OTf)$_2$.** This was synthesized according to modification of a literature procedure for [Pt(tpy)Cl](OTf)[S8] using [L][OTf] (219 mg, 0.41 mmol) instead of tpy. Yield = 300 mg (80 %). $^1$H NMR (400 MHz, DMSO-$d_6$): δ = 3.10(s, 9H), 4.64 (s, 2H), 7.85 (d, *J* = 8.2 Hz, 2H), 8.02 (m, 2H), 8.36 (d, *J* = 8.2 Hz, 2H), 8.60-8.62 (m, 2H), 8.89 (d, *J* = 8.7 Hz, 2H), 9.02 (d, *J* = 4.6 Hz, 2H), 9.09 (s, 2H). Positive FAB-MS, *m/z*: 761 $[M - OTf]^+$. Elemental analysis calcd (%) for $C_{27}H_{25}ClF_6N_4O_6PtS_2 \bullet H_2O$: C 34.94, H 2.93, N 6.04; found: C 35.21, H 2.95, N 6.05.

**Complex 1.** This was synthesized by dehydrohalogenation reaction of $[Pt(L)Cl](OTf)_2$ (300 mg, 0.33 mmol) and 1-ethynyl-3,5-dihydroxybenzene (134 mg,

1.0 mmol) in the presence of CuI (6 mg, 0.03 mmol) as the catalyst in DMF (10 mL) and distilled triethylamine (1 mL).[S9] After an overnight reaction, the solvent was removed by vacuum distillation. The crude product was dissolved in methanol-acetonitrile mixture and any undissolved solid was filtered off. The filtrate was evaporated under reduced pressure. Subsequent recrystallization by diffusion of diethyl ether vapour into a methanol-acetonitrile solution of complex **1** gave the product as a red solid. Yield = 100 mg (30 %). $^{1}$H NMR (400 MHz, DMSO-$d_6$, 333 K): δ = 3.10 (s, 9H), 4.68 (s, 2H), 6.18 (s, 1H), 6.35 (s, 2H), 7.84 (d, *J* = 8.0 Hz, 2H), 7.96 (m, 2H), 8.38 (d, *J* = 7.8 Hz, 2H), 8.55 (m, 2H), 8.84 (d, *J* = 7.8 Hz, 2H), 9.00-9.12 (br, 4H), 9.13 (d, *J* = 4.9 Hz, 2H); $^{13}$C{$^{1}$H} NMR (600 MHz, DMSO-$d_6$, 340 K): δ = 159.2, 158.5, 154.7, 154.6, 152.2, 142.4, 137.6, 134.2, 131.7, 130.1, 128.8, 128.1, 126.5, 122.1, 110.5, 105.1, 102.6, 97.4, 68.1, 52.8. IR (KBr disk, *v*/cm$^{-1}$): 2098 (w, C≡C), 1257 (s, C—O), 1165 (s, S=O). Positive FAB-MS, *m/z*: 859 [M – OTf]$^{+}$. Elemental analysis calcd (%) for $C_{35}H_{30}F_6N_4O_8PtS_2$: C 41.71, H 3.00, N 5.56; found: C 41.70, H 3.22, N 5.46.

**Complex 2.** The procedure was similar to that for complex **1** except that 4-ethynylphenol (117 mg, 1.0 mmol) was used instead of 1,3-dihydroxy-5-trimethylsilylethynylbenzene. The product was obtained as a red-purple solid. Yield = 125 mg (41 %). $^{1}$H NMR (400 MHz, DMSO-$d_6$, 333 K): δ = 3.11 (s, 9H), 4.67 (s, 2H), 6.76 (d, *J* = 8.5 Hz, 2H), 7.34 (d, *J* = 8.5 Hz, 2H), 7.85 (d, *J* = 8.4 Hz, 2H), 7.99 (m, 2H), 8.33 (d, *J* = 7.9 Hz, 2H), 8.57 (m, 2H), 8.86 (d, *J* = 7.9 Hz, 2H), 9.03 (s, 1H), 9.27 (d, *J* = 5.3 Hz, 2H), 9.60 (s, 2H); $^{13}$C{$^{1}$H} NMR (600 MHz, DMSO-$d_6$, 340 K): δ = 159.2, 156.8, 154.7, 152.1, 143.0, 142.4, 137.7, 134.2, 133.4, 131.5, 130.2, 128.8, 126.5, 122.1, 117.8, 115.7, 104.9, 95.8, 68.1, 52.8. IR (KBr disk, *v*/cm$^{-1}$): 2152 (w, C≡C), 1265 (s, C—O), 1172 (s, S=O). Positive FAB-MS,

*m/z*: 1069 [M + DMSO]$^+$. Elemental analysis calcd (%) for $C_{35}H_{30}F_6N_4O_7PtS_2$•EtOH: C 42.82, H 3.50, N 5.40; found: C 43.00, H 3.37, N 5.25.

**Complex 3.** The procedure was similar to that for complex **1** except that 1-ethynyl-3,5-dimethoxybenzene (178 mg, 1.0 mmol) was used instead of 1,3-dihydroxy-5-trimethylsilylethynylbenzene. The product was obtained as a dark red solid. Yield = 140 mg (41%). $^1$H NMR (400 MHz, DMSO-$d_6$, 353 K): δ = 3.23 (s, 9H), 3.80 (s, 6H), 4.68 (s, 2H), 6.46 (s, 1H), 6.71 (s, 2H), 7.87 (d, *J* = 8.2 Hz, 2H), 8.00 (m, 2H), 8.31 (d, *J* = 7.8 Hz, 2H), 8.55 (m, 2H), 8.86 (d, *J* = 7.8 Hz, 2H), 9.05 (s, 2H), 9.29 (d, *J* = 5.0 Hz, 2H); $^{13}$C{$^1$H} NMR (600 MHz, DMSO-$d_6$, 340 K): δ = 160.8, 159.1, 154.8, 154.7, 152.3, 142.5, 137.7, 134.2, 131.6, 130.3, 128.8, 128.5, 126.5, 122.1, 110.4, 104.6, 100.2, 99.0, 68.1, 55.8, 52.8. IR (KBr disk, *v*/cm$^{-1}$): 2106 (w, C≡C), 1257 (s, C−O), 1157 (s, S=O). Positive FAB-MS, *m/z*: 887 [M – OTf]$^+$. Elemental analysis calcd (%) for $C_{37}H_{34}F_6N_4O_8PtS_2$•EtOH: C 43.29, H 3.73, N 5.18; found: C 43.24, H 3.73, N 4.89.

**Measurements at different pH.** Electronic absorption and emission spectra of complexes **1**, **2** and **3** in aqueous solution (50 mM NaCl) were recorded at different pH by the addition of 0.02 M HCl or 0.02 M NaOH. The pH values were determined by a calibrated pH meter using standard buffer solutions of pH 4, 7 and 10. The ionic strength of the solutions was maintained by the presence of 50 mM NaCl.

**The dimerization plot for a monomer−dimer equilibrium of complex 1.**[S8a] With reference to the model reported in the literature:[S8a]

$$2\mathrm{Pt} \overset{K_{\pi\pi}}{\rightleftharpoons} (\mathrm{Pt_2})_{\pi\pi}$$
$$2\mathrm{Pt} \overset{K_{\mathrm{MM}}}{\rightleftharpoons} (\mathrm{Pt_2})_{\mathrm{MM}}$$

The dimerization equilibrium constants due to metal–metal and π–π interactions, $K_{MM}$ and $K\pi\pi$ respectively, can be determined from the following equation:[S8a]

$$\frac{[Pt]}{\sqrt{A}} = \frac{1}{\sqrt{\varepsilon_{MM} K_{MM}}} + \left(\frac{2}{\varepsilon_{MM}} + \frac{2K_{\pi\pi}}{\varepsilon_{MM} K_{MM}}\right)\sqrt{A}$$

where [Pt] is the concentration of complex **1**, $A$ is the absorbance of complex **1** at 670 nm and $\varepsilon_{MM}$ is the extinction coefficient of the MMLCT absorption band of the complex which is assumed to be 2000 $M^{-1}$ $cm^{-1}$ based on the reported values for Pt–Pt bonded dimers,[S10] similar to those reported in literature.[S8a]

**Determination of p$K_a$* of complexes 1 and 2.** The changes of the relative emission intensity of **1** and **2**, at 795 and 755 nm respectively, with pH were fitted to a sigmoid curve. The p$K_a$* of complex **1** and **2** were then determined from the pH where the relative emission intensity is equal to the mean of the maximum and minimum values, similar to other reported studies.[S11]

Although complex **1** contains two phenolic protons that can undergo deprotonation, the analysis of the emission spectral changes of **1** with pH only gave one single p$K_a$* value. Similar findings have been reported.[S11h]

**Protocol for fixed-cell confocal imaging with different intracellular pH.** MDCK cells were grown on a 35-mm tissue culture dish in the growth medium containing DMEM with 10% FBS and 1% penicillin/streptomycin and incubated at 37 $^{o}$C under a 5% $CO_2$ atmosphere. After the cells reached ~70 % confluence, the culture medium was removed, washed gently with PBS (1 mL × 3) and the cells were treated with pre-cooled methanol at –20 $^{o}$C for 10 min for fixation.[S12] After removal of the methanol solution, the fixed cells were washed gently with PBS (1 mL × 3), followed

by incubation with 20 μM of complex **1** in serum- and phenol red-free DMEM with 0.2 % DMSO for 1 h at 37 $^{o}$C under a 5% $CO_2$ atmosphere.

After the incubation with the complex solution, the medium was removed, washed gently with PBS (1 mL × 3) and replaced by the buffer solution of known pH. The buffer solutions contain 125 mM KCl, 20 mM NaCl, 0.5 mM $CaCl_2$, 0.5 mM $MgCl_2$, and 25 mM MES. The fixed cells were treated with the buffer solution for 10 min at room temperature and confocal imaging was then performed using a Leica TCS SPE confocal microscope with an excitation wavelength at 488 nm. The emission was measured at 750 ± 50 nm.

**Determination of NIR emission intensity from fixed MDCK cells at different intracellular pHs and the p$K_a$* value of complex 1 in the cells.** The confocal microscopy images of fixed MDCK cells at a particular intracellular pH were obtained at $\lambda_{ex}$ = 488 nm and $\lambda_{em}$ = 750 ± 50 nm. The total emission intensity in the region of interest (ROI) was found, and the NIR emission intensity from fixed MDCK cells at a particular pH was determined to be the average value of the emission intensities in the ROI obtained from at least 9 different images of the MDCK cells in at least 3 independent experiments at that particular pH value. The NIR emission intensity from fixed MDCK cells at other pHs were determined similarly using the ROI with the same area.

The NIR emission changes with intracellular pH were found to be fitted to a sigmoidal curve. Therefore, the p$K_a$* of complex **1** in the cells was similarly determined as that of the experiments in solution and in other reported studies.[S11]

**Protocol for confocal imaging of lysosomes in live-cells.** MDCK cells were grown on a 35-mm tissue culture dish in the growth medium containing DMEM with 10 %

FBS and 1 % penicillin/streptomycin and incubated at 37 $^{o}$C under a 5 % $CO_2$ atmosphere. After the cells reached ~70 % confluence, the culture medium was removed, washed gently with PBS (1 mL × 3) and replaced by 20 μM of complex **1** in serum- and phenol red-free DMEM with 0.2 % DMSO. After incubation at 37 $^{o}$C under a 5% $CO_2$ atmosphere for 1 h, the medium was removed, washed gently with PBS (1 mL × 3) and confocal imaging was then performed using a Leica TCS SPE confocal microscope with an excitation wavelength at 488 nm. The emission was measured at 750 ± 50 nm.

**Protocol for the determination of viability of cells by MTT assay.** MDCK cells were seeded in a 96-well flat-bottomed microplate (10000 cells/well) in the growth medium containing DMEM with 10 % FBS and 1 % penicillin/streptomycin (100 μL) and incubated at 37 $^{o}$C under a 5 % $CO_2$ atmosphere. After 24 h incubation, the culture medium was removed and replaced by 20 μM of complex **1** in serum- and phenol red-free DMEM with 0.2 % DMSO (100 μL), with wells containing MDCK cells in serum- and phenol red-free DMEM without complex **1** as the control. The microplate was incubated for desired time intervals and the same conditions as the cell-imaging experiments. Then 10 μL of MTT in PBS (5 mg $mL^{-1}$) was added to each well and the microplate was further incubated at 37 $^{o}$C under a 5 % $CO_2$ atmosphere for 3 h. After that the medium was removed carefully and DMSO (200 μL) was added to each well. The absorbance of all the solutions at 570 nm was measured with a SPECTRAmax 340 microplate reader (Molecular Devices Corporation, Sunnyvale, CA). The viability of cells in the cell-imaging experiments was then estimated to be the ratio of the absorbance at 570 nm of the DMSO solutions from the MDCK cells incubated with complex **1** to the absorbance of the control (DMSO solutions from MDCK cells without incubation with complex **1**).

**Protocol for co-staining experiments with LysoSensor Green DND-189.** Before the imaging experiments, the culture medium was removed, the cells were washed gently with PBS (1 mL × 3) and then incubated in 1 μM of DND-189 in serum- and phenol red-free DMEM with 0.1 % DMSO. After incubation at room temperature for 15 min, the medium was removed, the cells were washed gently with PBS (1 mL × 3) and confocal imaging was then performed with $\lambda_{ex}$ = 488 nm and $\lambda_{em}$ = 750 ± 50 nm for the NIR emission of complex **1** and $\lambda_{em}$ = 525 ± 25 nm for the green emission of DND-189. The Mander's colocalization coefficient of the NIR emission of complex **1** with the green emission of DND-189 was determined from the image correlation analysis by WCIF ImageJ.

In summary, serum- and phenol red-free DMEM was used during the incubation of MDCK cells with complexes **1** and, **3**, and LysoSensor DND-189, as well as further incubation, if needed, after the loading of MDCK cells with complexes **1** and **3**.

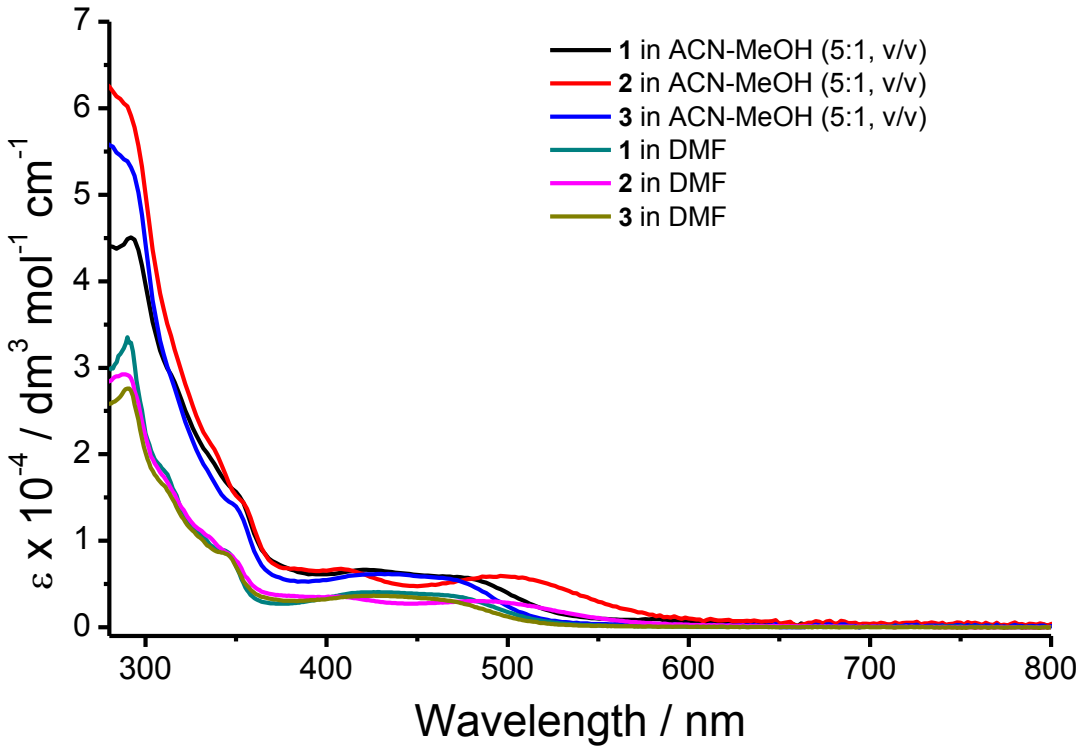


**Fig. S1** Electronic absorption spectra of complexes **1**–**3** in acetonitrile-methanol (5:1, v/v) solution mixture and DMF solution at 298 K.

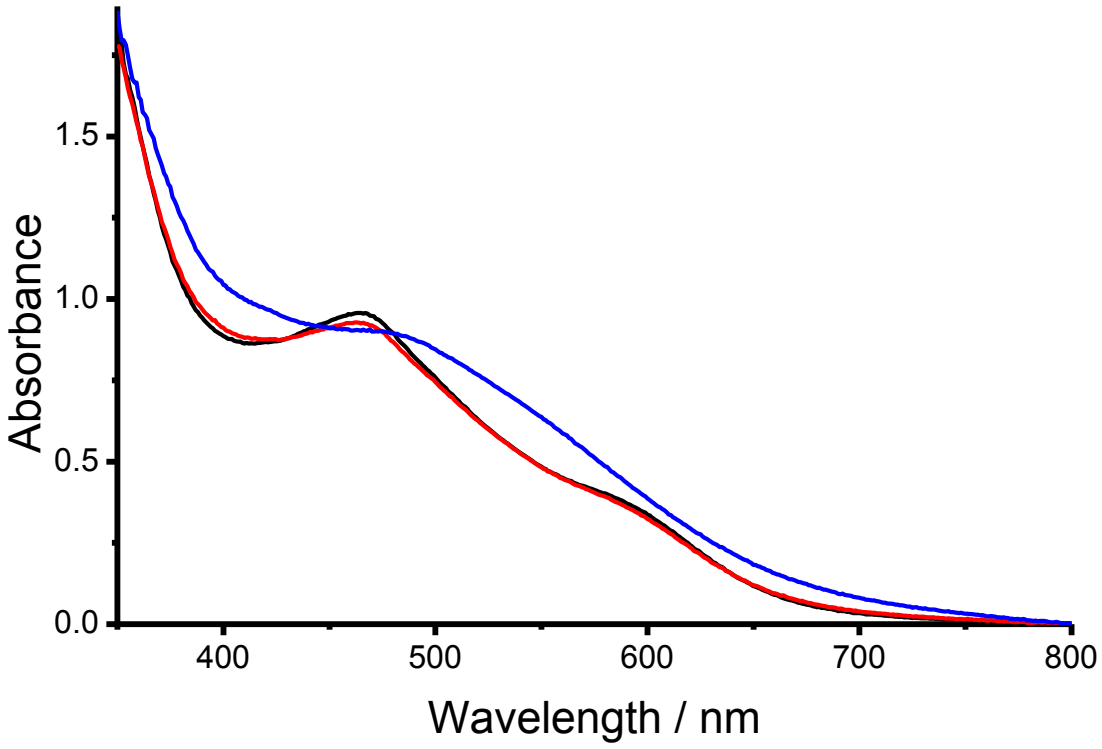


**Fig. S2** Electronic absorption spectra of complex **1** (200 μM) in aqueous solution (50 mM NaCl) at (black) pH 4, (red) 7 and (blue) 10.

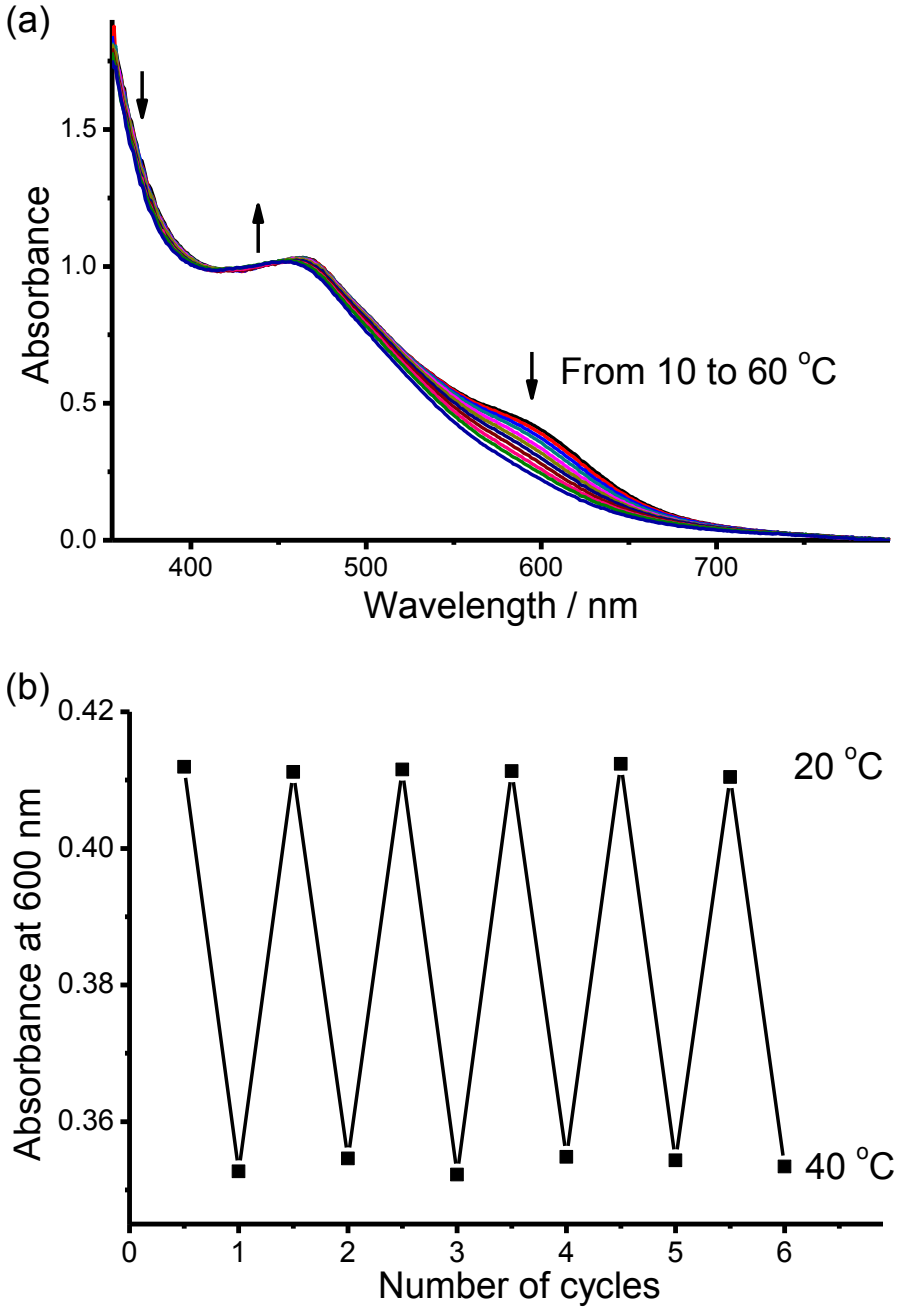


**Fig. S3** (a) The electronic absorption spectral changes of complex **1** (200 μM) in aqueous solution (50 mM NaCl) with increasing temperature at pH 4. (b) The electronic absorption spectral changes of complex **1** (200 μM) in aqueous solution (50 mM NaCl) at pH 4 with six cycles of heating and cooling.

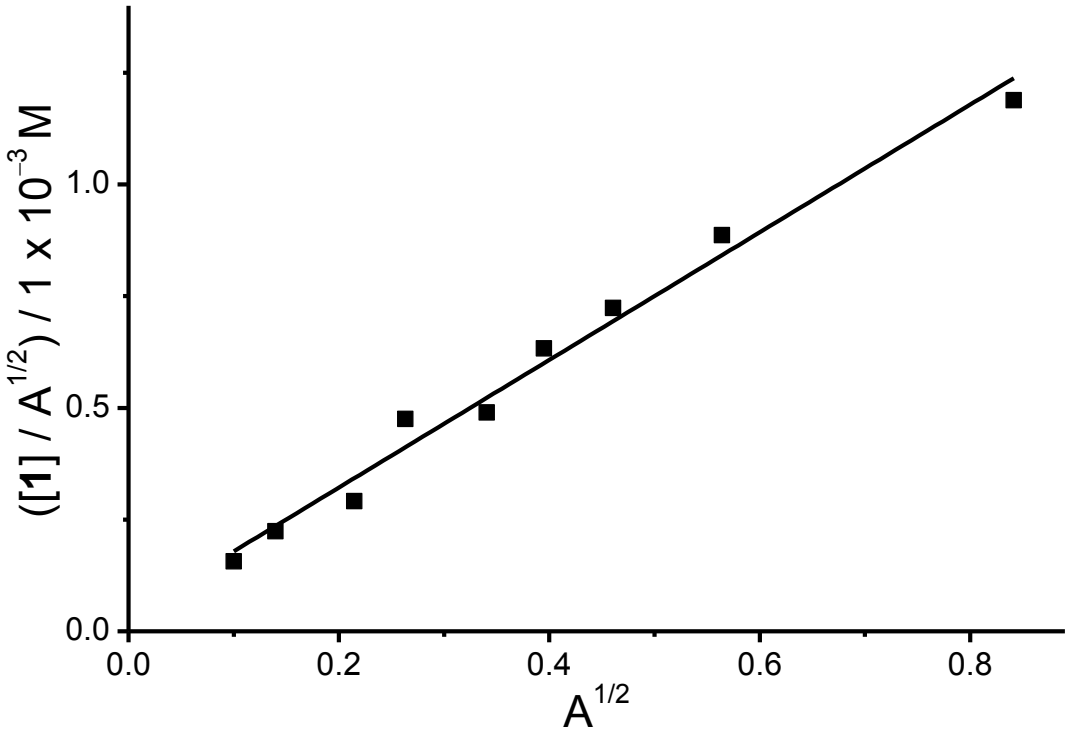


**Fig. S4** Dimerization plot for a monomer−dimer equilibrium for complex **1** in aqueous solution (50 mM NaCl) at pH 4 monitored at 670 nm.

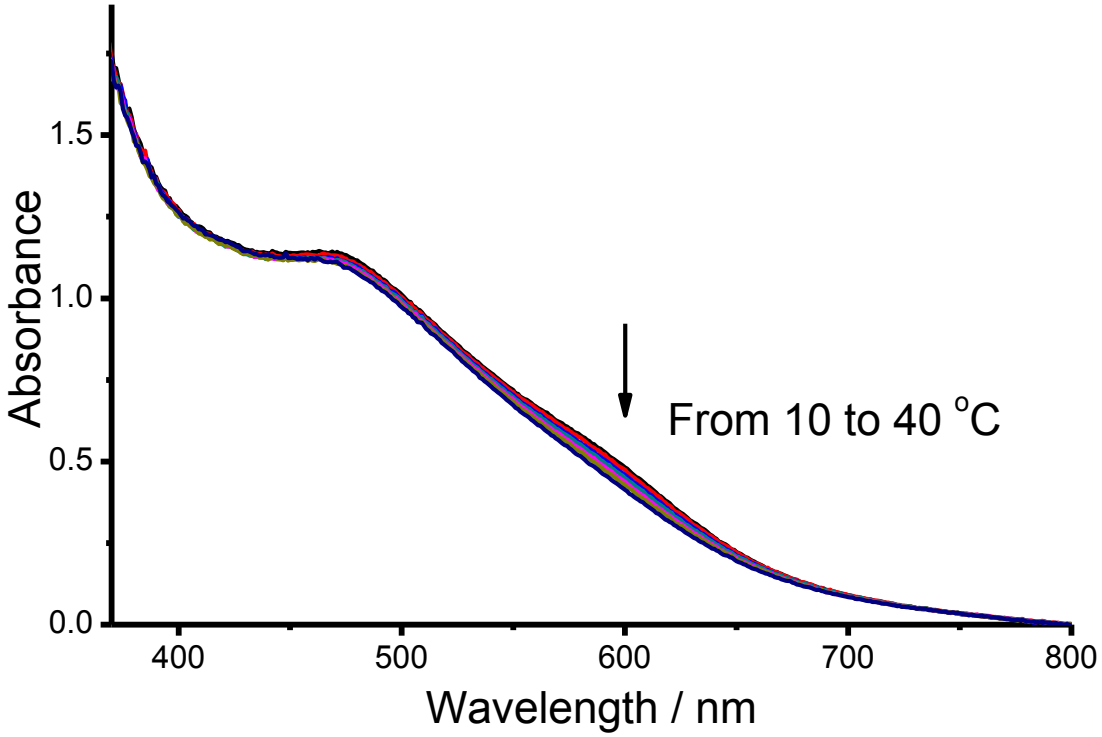


**Fig. S5** The electronic absorption spectral changes of complex **1** (200 μM) in aqueous solution (50 mM NaCl) with increasing temperature at pH 10.

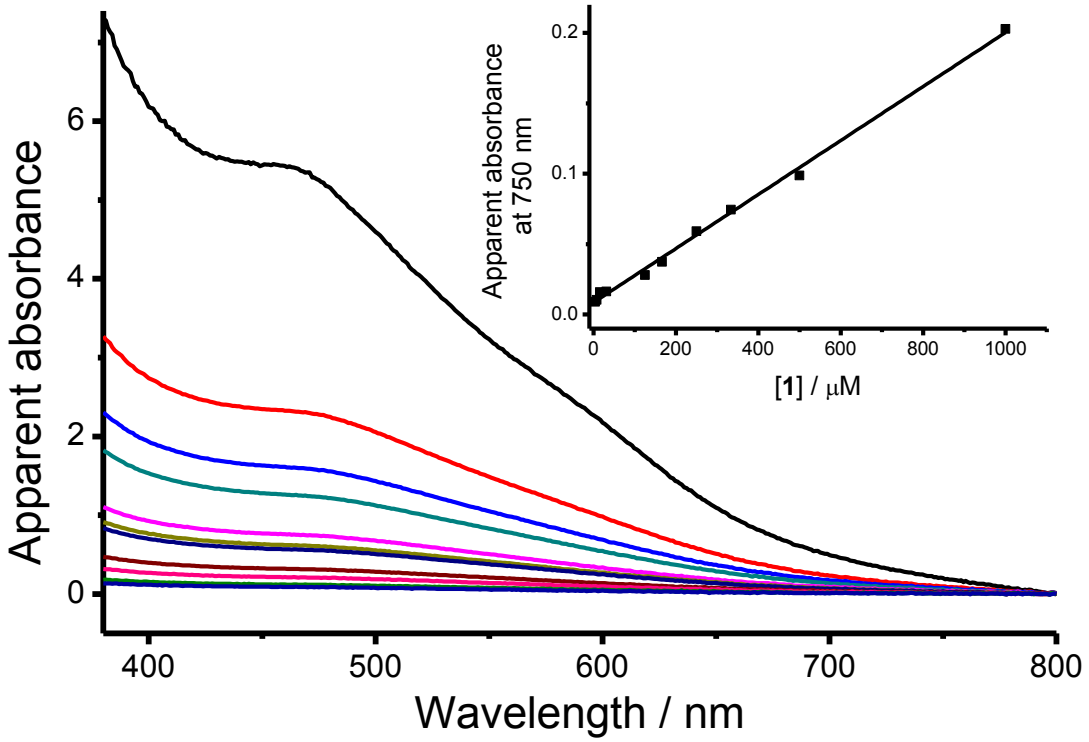


**Fig. S6** Concentration-dependent UV−vis absorption spectra of complex **1** (200 μM) in aqueous solution (50 mM NaCl) at pH 10. The absorbance values have been corrected to 1 cm path length equivalence. Inset shows the plot of apparent absorbance at 750 nm against concentration of complex **1**.

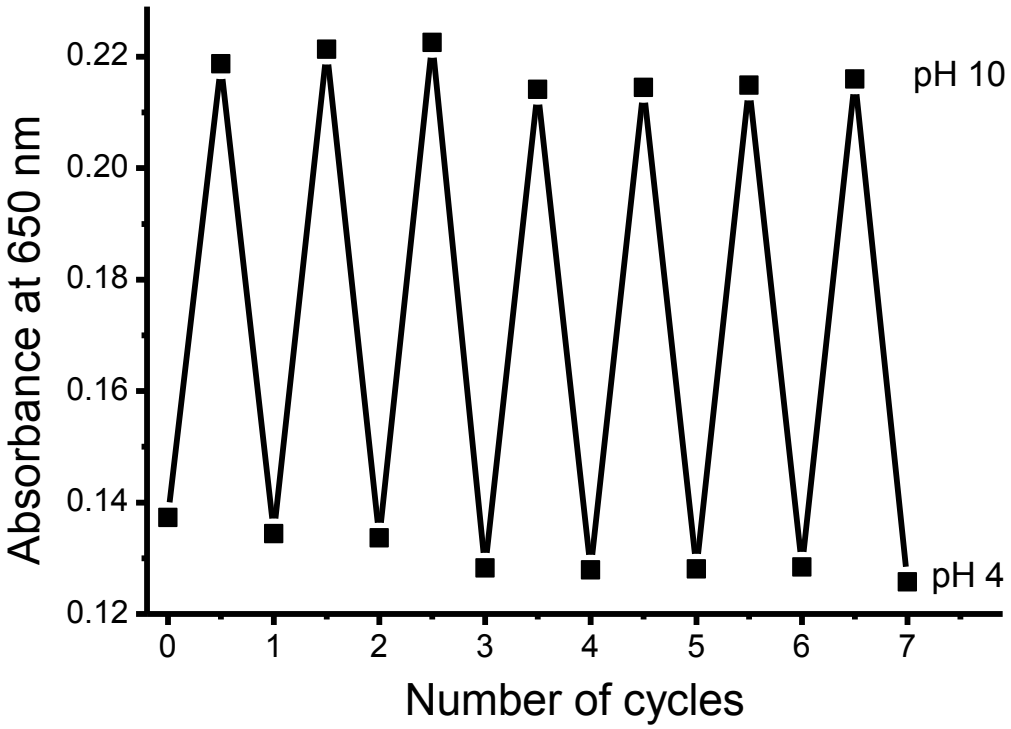


**Fig. S7** The changes in absorbance of complex **1** (200 μM) in aqueous solution (50 mM NaCl) at 650 nm with seven cycles of pH switching between 4 and 10.

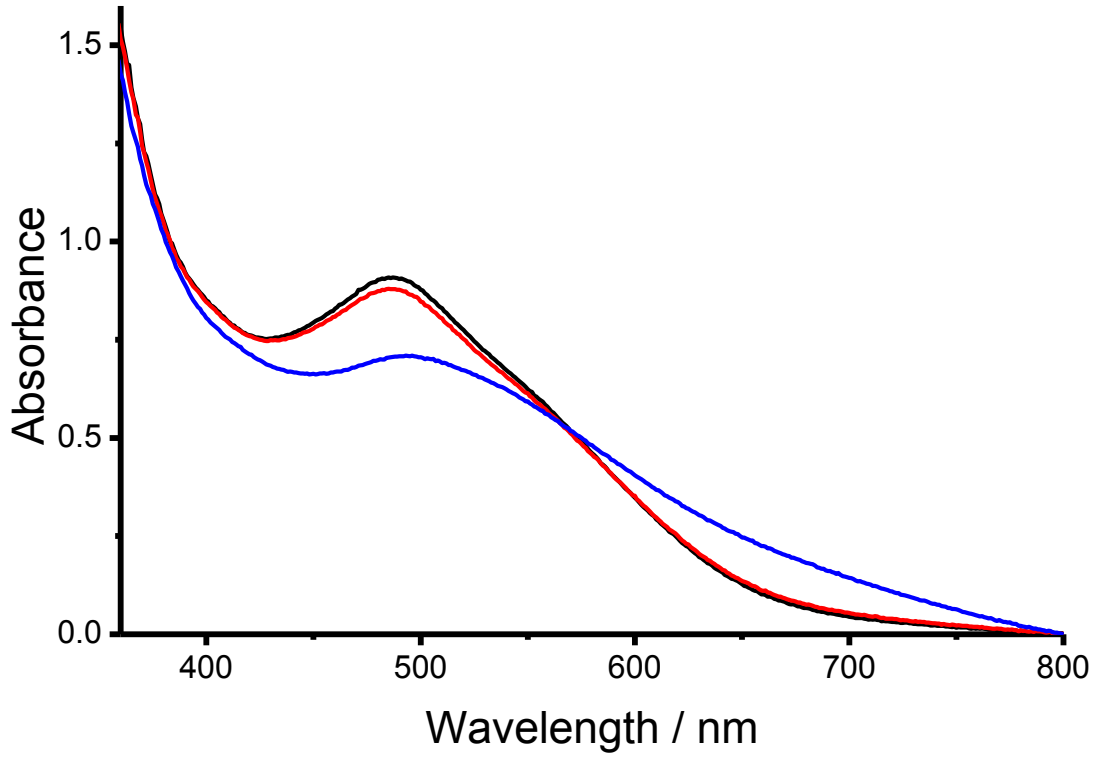


**Fig. S8** Electronic absorption spectra of complex **2** (200 μM) in aqueous solution (50 mM NaCl) at (black) pH 4, (red) 7 and (blue) 10.

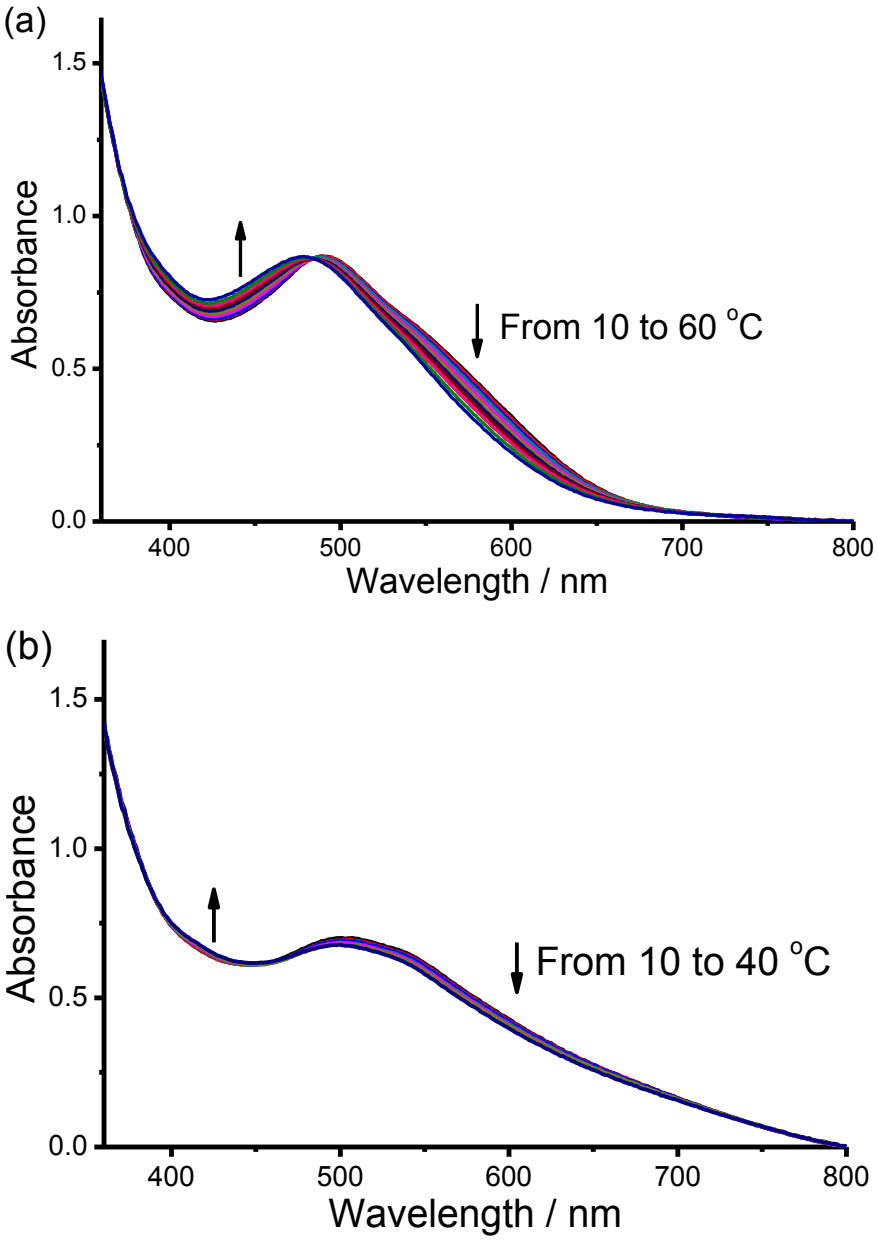


**Fig. S9** The electronic absorption spectral changes of complex **2** (200 μM) in aqueous solution (50 mM NaCl) with increasing temperature at (a) pH 4 and (b) pH 10.

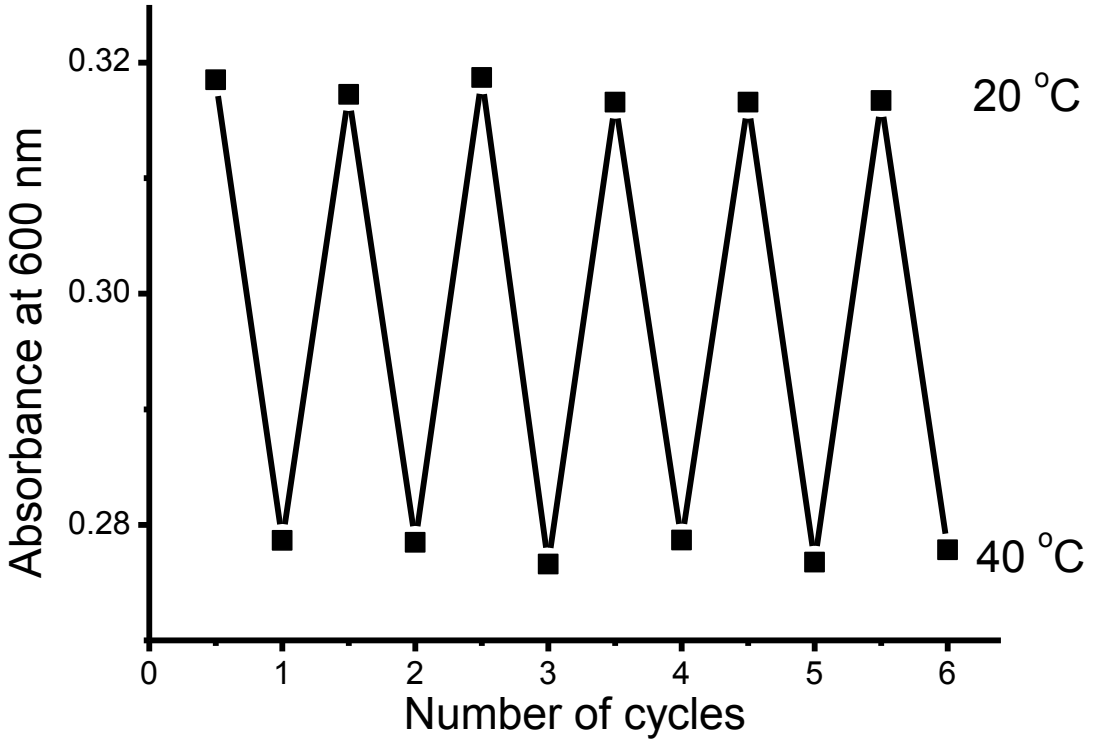


**Fig. S10** The electronic absorption spectral changes of complex **2** (200 μM) in aqueous solution (50 mM NaCl) at pH 4 with six cycles of heating and cooling.

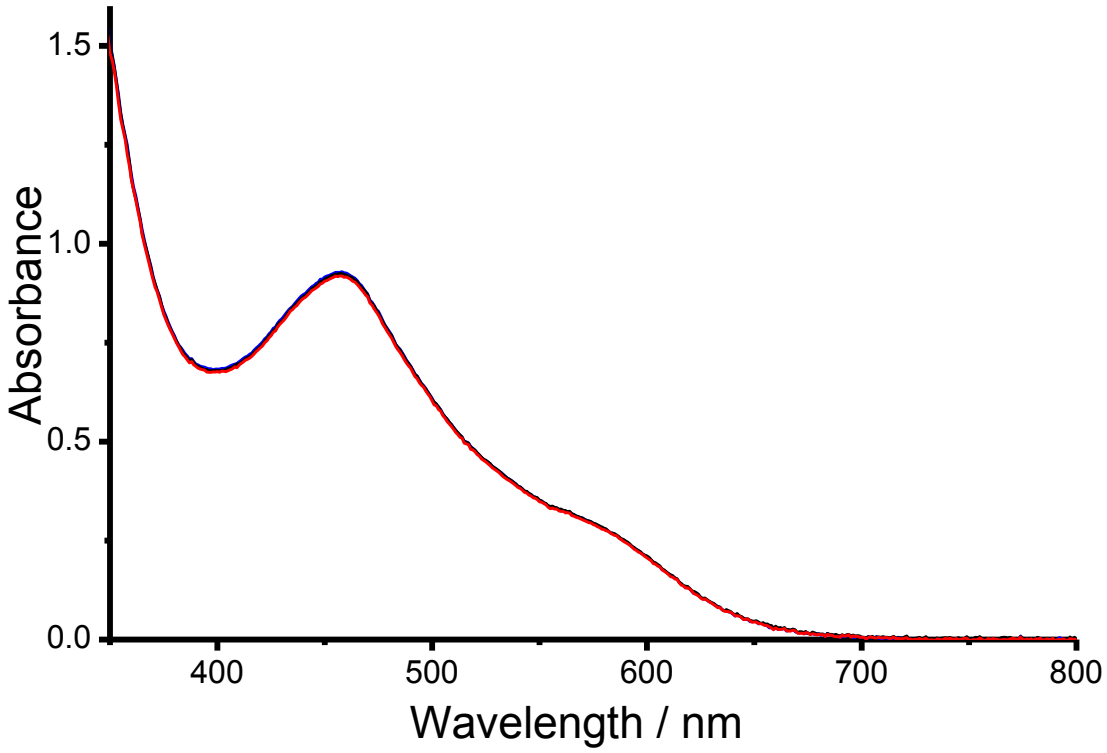


**Fig. S11** Electronic absorption spectra of complex **3** (200 μM) in aqueous solution (50 mM NaCl) at (black) pH 4, (red) 7 and (blue) 10.

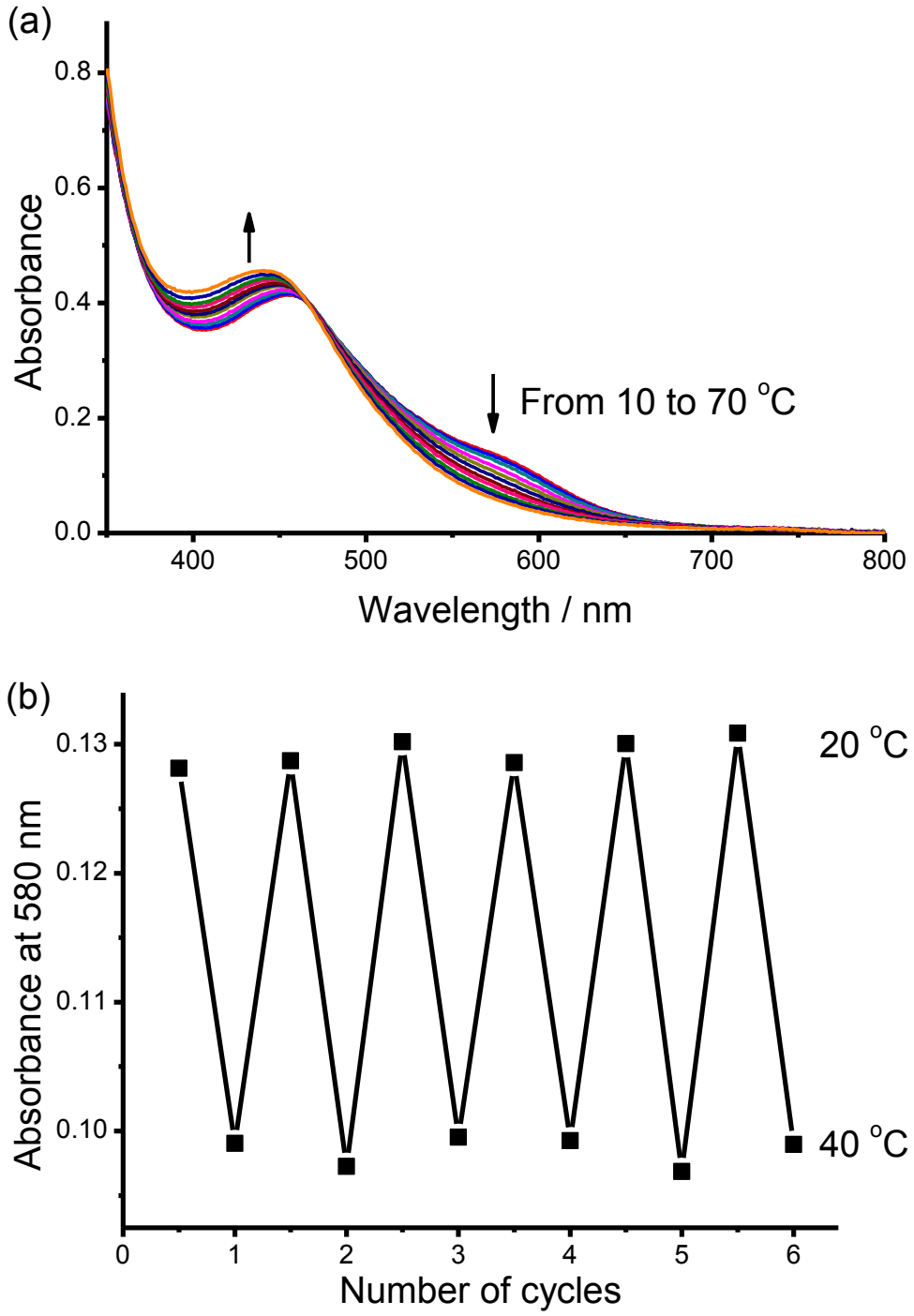


**Fig. S12** (a) The electronic absorption spectral changes of complex **3** (200 μM) in aqueous solution (50 mM NaCl) with increasing temperature at pH 7. (b) The electronic absorption spectral changes complex **3** (200 μM) in aqueous solution (50 mM NaCl) at pH 4 with six cycles of heating and cooling.

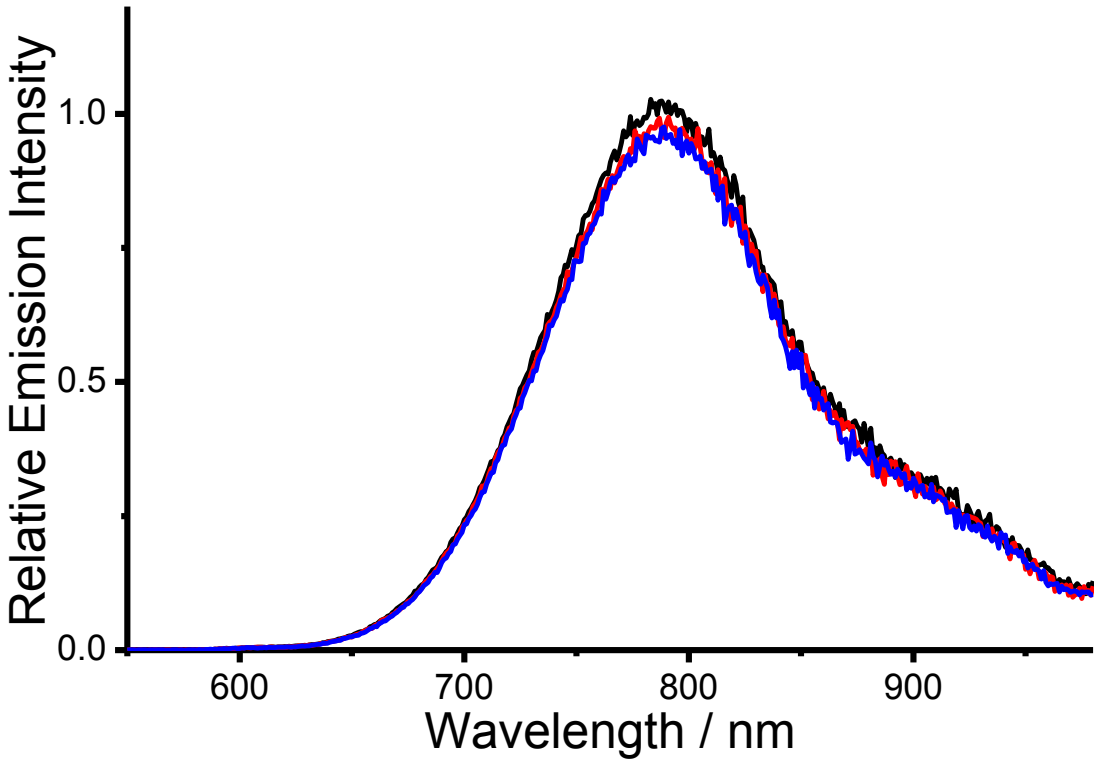


**Fig. S13** Emission spectra of complex **3** (200 μM) in aqueous solution (50 mM NaCl) at 25 $^{o}$C at pH (black) 4, (red) 7 and (blue) 10. Excitation was at 480 nm.

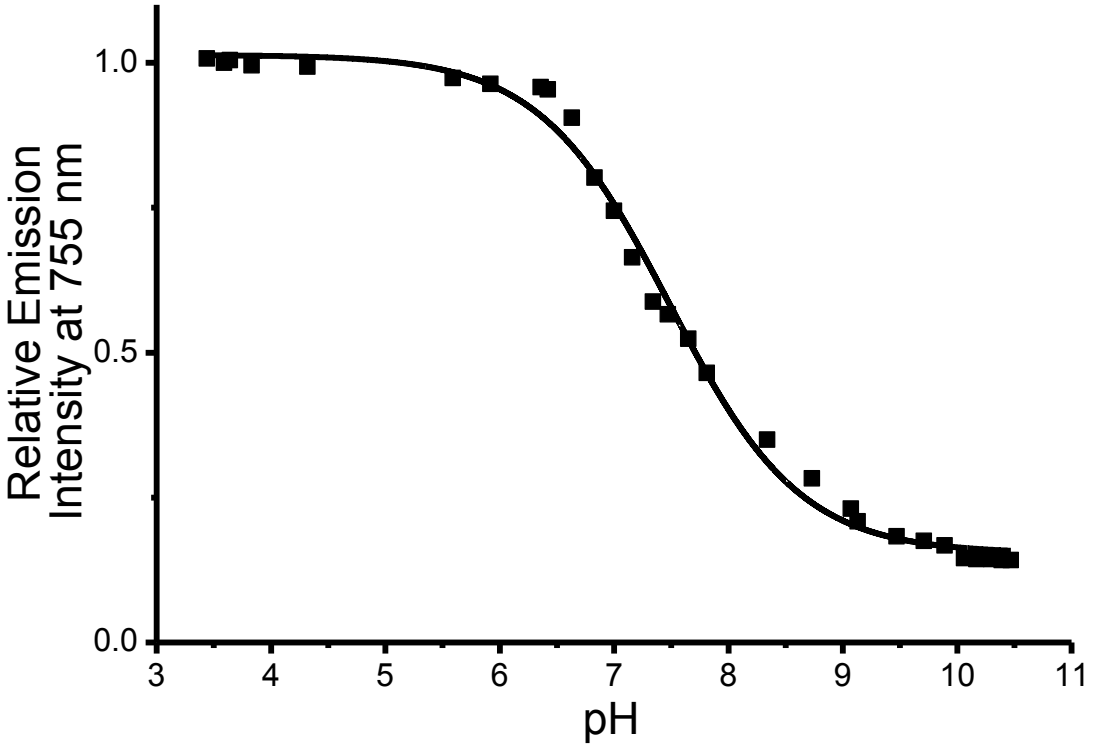


**Fig. S14** A plot of relative emission intensity of complex **2** in aqueous solution (50 mM NaCl) at 755 nm against pH. Excitation was at 380 nm.

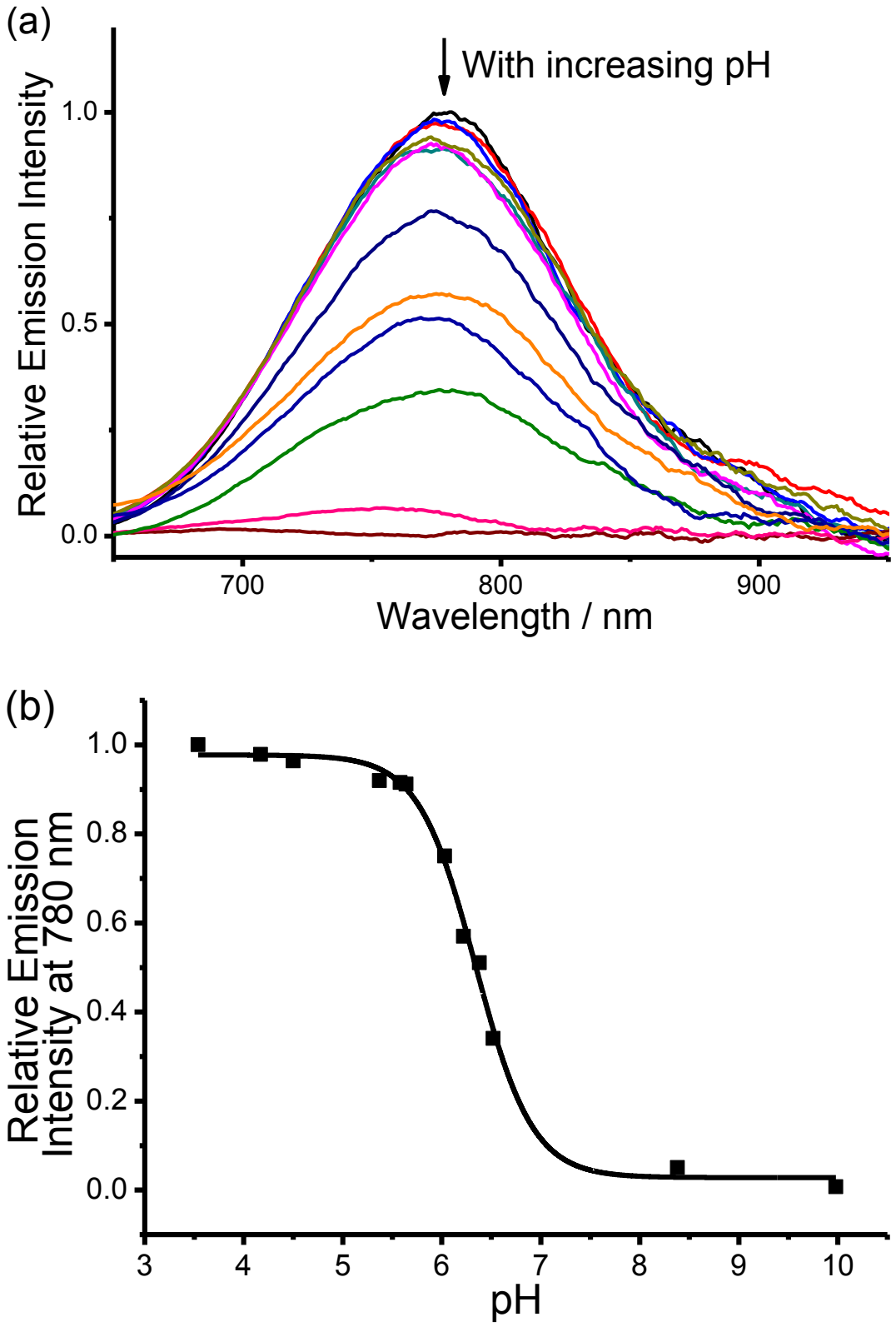


**Fig. S15** (a) Emission spectra of complex **1** (20 μM) in aqueous solution (50 mM NaCl) at different pHs at 25 $^{o}$C. Excitation was at 480 nm. (b) A plot of relative emission intensity of complex **1** at 780 nm against pH.

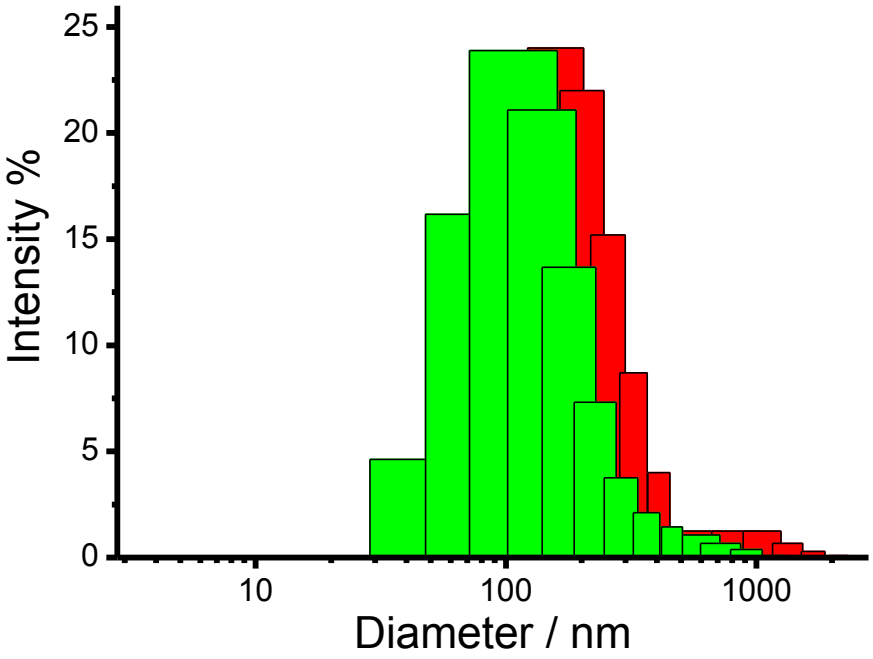


**Fig. S16** Dynamic light scattering (DLS) experiments of complex **1** (20 μM) in aqueous solution (50 mM NaCl) at 25 $^{o}$C at pH 4 (red) and pH 10 (green). The solution at pH 4 was found to form aggregates with number-averaged hydrodynamic diameter ($D_h$) of *ca*. 210 (major signal in the DLS experiment) and 990 nm (minor signal) respectively, while $D_h$ of pH 10 aqueous solution was found to be *ca*. 160 nm.

**Table S1 Electrochemical data of complexes 1−3 at 298 K**

| Complex | Oxidation | Reduction |
|---|---|---|
| | $E_{1/2}$[a]/V vs SCE ($\Delta E_p$/mV) | $E_{1/2}$[a]/V vs SCE ($\Delta E_p$/mV) |
| | [$E_{pa}$[b]/V vs SCE] | [$E_{pc}$[c]/V vsSCE] |
| **1**[d] | +0.42 (60) | −0.81 (63) |
| | [+0.97] | [−1.25] |
| | [+1.15] | −1.34 (72) |
| **1**[e] | +0.42 (62) | −0.81 (66) |
| | [+0.61] | [−1.23] |
| | [+1.06] | −1.34 (69) |
| **2**[d] | +0.42 (67) | −0.83 (71) |
| | [+0.73] | [−1.23] |
| | [+1.00] | −1.33 (71) |
| **2**[e] | +0.42 (60) | −0.83 (61) |
| | [+0.55] | [−1.24] |
| | [+0.84] | −1.34 (70) |
| **3**[d] | +0.42 (60) | −0.77 (67) |
| | [+1.29] | [−1.24] |
| | | −1.33 (60) |

[a] $E_{1/2} = (E_{pa} + E_{pc})/2$; $E_{pa}$ and $E_{pc}$ are anodic peak and cathodic peak potentials, respectively. [b] $E_{pa}$ refers to the anodic peak potential for the irreversible oxidation waves. [c] $E_{pc}$ refers to the cathodic peak potential for the irreversible reduction waves. [d] In dimethylformamide solution with 0.1 M $^n$Bu$_4$NPF$_6$ as supporting electrolyte; scan rate 100 mV s$^{-1}$. [e] In dimethylformamide solution with 0.1 M $^n$Bu$_4$NPF$_6$ as supporting electrolyte and $^n$Bu$_4$NOH (50 μM); scan rate 100 mV s$^{-1}$.

**References:**


S1. J. Wang and G. S. Hanan, *Synlett*., 2005, **8**, 1251.

S2. J. M. Haider, M. Chavarot, S. Weidner, I. Sadler, R. M. Williams, L. D. Cola and Z. Pikramenou, *Inorg. Chem.*, 2001, **40**, 3912.

S3. C. Gottardo and A. Aguirre, *Tetrahedron Lett*., 2002, **43**, 7091.

S4. J. Zhao and R. C. Larock, *J. Org. Chem.*, 2006, **71**, 5340.

S5. H. Zhao, Y. Wang, J. Sha, S. Sheng and M. Cai, *Tetrahedron*, 2008, **64**, 7517.

S6. J. Chen, J. W. Kampf and A. J. McNeil, *Langmuir*, 2010, **26**, 13076.

S7. J. T. Wang, Y. Li, J. H. Tan, L. N. Jia and Z. W. Mao, *Dalton Trans.*, 2011, **40**, 564.

S8. (a) J. A. Bailey, M. G. Hill, R. E. Marsh, V. M. Miskowski, W. P. Schaefer and H. B. Gray, *Inorg. Chem.*, 1995, **34**, 4591; (b) G. T. Morgan and F. H. Burstall, *J. Chem. Soc.*, 1934, 1498; (c) M. Howe-Grant and S. J. Lippard, *Inorg. Synth.*, 1980, **20**, 101.

S9. (a) K. Sonogashira, S. Takahashi and N. Hagihara, *Macromolecules*, 1977, **10**, 879; (b) S. Takahashi, M. Kariya, T. Yakate, K. Sonogashira and N. Hagihara, *Macromolecules*, 1978, **11**, 1063; (c) V. W. W. Yam, C. H. Tao, L. Zhang, K. M. C. Wong and K. K. Cheung, *Organometallics*, 2001, **20**, 453.

S10. J. A. Bailey, V. M. Miskowski and H. B. Gray, *Inorg. Chem.*, 1993, **32**, 369.

S11. (a) Z. J. Myng and P. Gabor, *Anal. Chem.*, 1991, **63**, 2934; (b) M. S. Briggs, D. D. Burns, M. E. Cooper and S. J. Gregory, *Chem. Commun.*, 2000, 2323; (c) O. Finikova, A. Galkin, V. Rozhkov, M. Cordero, C. Hägerhäll and S. Vinogradov, *J. Am. Chem. Soc.*, 2003, **125**, 4882; (d) Z. Zhang and S. Achilefu, *Chem. Commun.*, 2005, 5887; (e) S. A. Hilderbrand and R. Weissleder, *Chem. Commun.*, 2007, 2747; (f) B. Tang, X. Liu, K. H. Xu, H. Huang, G. W. Yang and L. G. An, *Chem. Commun.*, 2007, 3726; (g) A. Almutairi, S. J. Guillaudeu, M. Y. Berezin, S. Achilefu and J. M. J. Fréchet, *J. Am. Chem. Soc.*, 2008, **130**, 444; (h) B. Tang, F. Yu, P. Li, L. Tong, X. Duan, T. Xie and X. Wang, *J. Am. Chem. Soc.*, 2009, **131**, 3016; (i) S. Thyagarajan, T. Leiding, S. P. Årsköld, A. V. Cheprakov and S. A. Vinogradov, *Inorg. Chem.*, 2010, **49**, 9909.

S12. (a) J. Epstein, H. Xiao and B. K. Oba, *Blood*, 1989, **74**, 913; (b) A. A. Pollice, J. P. McCoy, Jr., S. E. Shackney, C. A. Smith, J. Agarwal, D. R. Burholt, L. E. Janocko, F. J. Hornicek, S. G. Singh and R. J. Hartsock, *Cytometry*, 1992, **13**, 432; (c) M. Dasari, S. Lee, J. Sy, D. Kim, S. Lee, M. Brown, M. Davis, N. Murthy, *Org. Lett.*, 2010, **12**, 3300; (d) U. Schnell, F. Dijk, K. A. Sjollema and B. N. G. Giepmans, *Nat. Methods*, 2012, **9**, 152.